Jestr

Journal of Engineering Science and Technology Review 15 (1) (2022) 177 - 184

JOURNAL OF
Engineering Science and Technology Review

Research Article

www.jestr.org

Experimental Study of The Design of Axial Flux Permanent Magnet Generator Using Layers of Rectangular NDFEB Magnet for Small Wind Power Applications

Sudirman Syam* and Sri Kurniati

Electrical Engineering Department, Science and Engineering Faculty, University of Nusa Cendana, Kupang, Indonesia

Received 5 January 2021; Accepted 10 April 2022

Abstract

In this paper, the design and manufacturing process of axial flux permanent magnet (AFPM) generators using rectangular neodymium ferrite boron (NdFeB) magnets are described to reduce magnet costs. Experimental studies are carried out by measuring the output voltage based on the design that has been made. The process of making a generator is made by varying the magnetic bars parallel and layered. Emphasis is placed on using commercially available rectangular magnetic teeth with simple techniques to achieve lower costs, while the fabrication steps in the manufacturing process are described in more detail. The design and prototype of the built AFPM generator are laboratories tested. The experimental study results obtained by the number of stator windings as many as 324 turns with an arrangement of 4 rectangular magnetic layers obtained an output voltage of 13.1 Volt at 1400 rpm. In addition, the structure of the generator design is simple and easy to manufacture and is suitable for rural applications for small-scale energy turbine applications.

Keywords: Wind energy, NdFeB permanent magnet, Axial machine

1. Introduction

Currently, permanent magnet (PM) machines have replaced other electric machines in various applications [1,2]. The higher reliability of PM materials, higher energy density, greater corrosion resistance, and the effect of demagnetization were the main causes of the development of PM generators. Many PM generators have been used and proposed to convert wind energy, such as radial, axial and transverse flux. Several researchers have conducted comparative studies of these types based on technology and manufacturing; some work has been done using different comparison procedures [3–5]. Transverse flux engines are known for their higher torque density, but their electromagnetic structure is more complicated than radial and axial flux engines. Axial flux engines are known to have a higher torsion density than their counterparts based on radial flux. While [6] has reported a comparison procedure with consideration of heat at the same volume size, surface losses per unit, air gap, magnetic gear, yoke flux density and rotational speed of the two machine structures, and the influence of pole numbers. The advantage of the axial permanent magnet flux (AFPM) engine's torque density becomes more pronounced in designs with a large number of poles.

The technology of making stator slots in radial flux PM machines is well known in the industry and is therefore widely used by generator manufacturers. However, the manufacture of stator slots will require special equipment to manufacture, which may not be available in many developing countries, especially in rural areas. Therefore, the process of manufacturing such a special slot for the stator winding is not suitable for building a generator in a small workshop. Slot creation is even more difficult on AFPM machines, potentially increasing the cost of creating them. For this reason, the AFPM type is not as popular as the radial flux type but is increasingly in demand by researchers [7-10]. The AFPM machine is formed by a rotor disc carrying magnet, which produces an axial flux, and a stator disc containing the phase windings. In recent years, several types of variations in this basic design have been possible, including single-sided with one rotor and one perforated stator [11], double-sided with slot-less (coreless) cores [7, 8, 10, 12], torus [13-19], AFIR-NS [20], AFIR-S [21-23], and multi-disk designs [24]. However, each design has its complexity in the prototype and design of the magnet gear, especially for wind power generation. Several parameters must be considered in redesigning the generator for higher voltage output. It includes the number of poles, the magnetic flux field density, the number of turns of the coil, the resistance of the wire, the maximum current, and the space available in the armature coil.

On the other hand, the main requirements for designing wind generators are simple construction, low cost, lighter weight, low speed, and high output power. Small AFPM generators can play an important role in domestic or small business applications, especially in rural areas. Given the limited access to start-up capital in most rural applications worldwide, minimizing total application costs is critical. That can be achieved by minimizing material costs and simplifying the manufacturing process. Various design construction manuals for small wind turbines with nominal power up to 3 kW can be found [25]. There is some literature on AFPM generator prototypes for small wind turbine applications, such as the use of coin magnets [1, 26], sectoral magnets [28], and wood materials for stator disks [27]. Generally, sectoral-shaped magnets are applied in the rotor of the AFPM generator. In addition, there are inherent problems such as high prices and supply shortages. Therefore, the main concern of this design was the replacement of coin magnets and sectoral magnets with rectangular magnets. In this case, rectangular magnets are solutions in the fabrication of AFPM

*E-mail address: sudirman_s@staf.undana.ac.id
ISSN: 1791-2377
doi:10.25103/jestr.151.22

generators for small wind turbines. According to [29], compared to sectoral magnets, rectangular magnets are cheaper, and dimensional materials are available. Geometrically, rectangular magnets have advantages, low production costs, and easy magnetization [30].

In connection with the manufacture of a simple and inexpensive AFPM machine, this paper proposes a new structure of rotor magnet teeth using rectangular NdFeB magnets. An engineering use of rectangular magnets arranged in 4 layers aims to increase the magnetic flux. According to [31], the arrangement of rectangular magnets in layers is the same as that of parallel magnet circuits. Analytical approximation, in a magnetic circuit, resistance (R) and reluctance (ℜ) are inversely proportional to area, showing that increasing the surface area will result in a decrease in value and will increase the desired results in terms of current and flux [32].

2. Fundamentals of Machine Design

2.1 Rotor PM Design

The configuration of the AFPM machine consists of an external rotor and an internal air-core stator (coreless). The design calculations for AFPM engines with air-core stators using the sizing equations are described in this section. The magnetic design model is based on the single-disc eight-pole AFPM shown in Fig. 1. It is used to calculate engine parameters and further analyze and optimize engine performance. The magnetic flux flows straight across the air gap between the stator and rotor. The total flux through the same magnetic surface area does not change, and the air-gap flux density is flat and constant in the radial direction.

Considering a single-phase machine with eight windings in a 360-degree section of electricity, the magnetic circuit of a flux loop consists of one winding on each side of the stator, facing two parallel permanent magnets embedded in the rotor. The magnetic circuit model for one electric period for the motor half is expressed in air gap reluctance, stator magnetic force, and flux through the magnetic circuit. The area of the rotor circumference based on the rectangular magnetic arrangement as a source of magnetic flux excited by PMs per pole is defined as follows:

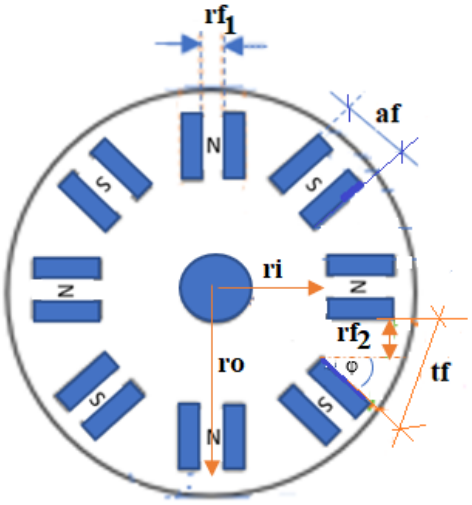

Fig. 1. Rotor disc

The distance between the same pole magnets is obtained:

$$af = (2\ x\ a) + rf_1 \quad (1)$$

while the distance between the magnets with different poles is:

$$tf = (Sin\ \varphi\ x\ b) + rf2, \quad \varphi = 45^0 \quad (2)$$

Thus, the circumference of the rotor is obtained by Eq. (3):

$$Cf = (Tf\ x\ p) + (af\ x\ p) \quad (3)$$

The inner radius (ri) and outer radius (ro) of the rotor disk are obtained:

$$r_o = \frac{Cf}{2\pi} \quad (4)$$

$$r_i = r_o - b \quad (5)$$

where:

a = width of the magnet, and
b = length of magnet
rf = the air gap between the poles of the same magnet
af = distance between the same pole magnets
tf = distance between the magnets with different poles
p= number of poles
Cf= circumference of the rotor
ro= outer radius
ri= inner radius

2.2 Design Equation for AFPMSG with Slotless Stator

The calculation of the air-core stator design of the AFPM generator is shown in Fig. 2.

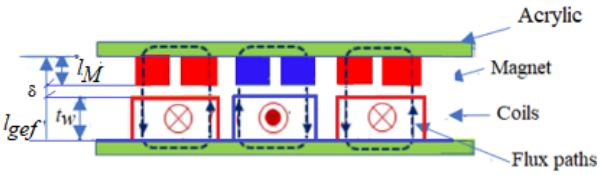

Fig. 2. Geometry and flux path in air-gap

The effective air gap (l_{gef}) for the machine can be calculated by the following Eq. (6).

$$l_{gef} = \delta \frac{l_m}{\mu_r} + t_w \quad (6)$$

To determine the maximum magnetic flux, it is determined by Eq. (7):

$$B_{maks} = B_r \frac{l_m}{l_m + \delta}, \quad (7)$$

where:

Br = flux density (T)
lm = thickness of magnet (m)
δ = width of air gap (m)

In determining the area of the magnet (*Am*), where the rotor and stator disk areas are the same, Eq. (8) is used.

$$A_m = \frac{\pi\,(r_0^2 - r_i^2) - rf\,(r_0 - r_i)p}{p} \quad (8)$$

Based on Eqs. (7) and (8) it can be calculated the maximum flux value using Eq. (9) as follows,

$$ø_{max} = A_m \times B_{max} \quad (9)$$

Furthermore, for the number of turns on the generator stator, Eqs. (10) and (11):

$$N = \frac{E}{4{,}44\ x\ f\ x\ K_{W1} x\ \phi} \quad (10)$$

Number of turns/poles,

$$\sum N_p = \frac{P}{Number\ of\ turn} \quad (11)$$

where:

ΣN_p = number pf turns/poles
P = number of poles
E = phase voltage (V)
f = frequency (Hz)
k_{w1} = winding factor (0,8)
ϕ = magnetic flux (Wb)

The generator output power can be calculated by,

$$P_{out} = E.I.cosØ \quad (12)$$

The input power of the generator is given by the following equation,

$$P_{in} = P_{out} + Losses \quad (13)$$

The efficiency of the generator can be calculated by,

$$\eta = \frac{P_{out}}{P_{in}} x100\% \quad (14)$$

The mechanical design parameters of the slotless AFPM generator are shown in Table 1.

Table 1. Main parameters of the AFPM Generator prototype

Parameters	Symbol	Value
PM axial length, mm	b	20
PM width, mm	a	10
PM thickness, mm	lm	1
The air gap distance between the poles of the same PM, mm	rf_1	10
The air gap distance between the poles of the different PM, mm	rf_2	20
Distance between the same pole PM, mm	Af	25
Distance between the poles of the different PM, mm	Tf	28.28
The circumference of the rotor, mm	Cf	513.12
Outer radius of rotor, mm	Ro	81.7
Inner radius of rotor, mm	Ri	61.7
Number of poles	P	8
Air gap distance between rotor and stator (Adjustable), mm	δ	1 – 4
Frequency, Hz	F	50
The maximum magnetic flux, T	Br_{max}	1.8
The number of turns per coil, turns	N	117

3. Basics on Design Procedure

The dimensioning of the machine prototype is carried out iteratively through an analytical approach based on several simplifying assumptions. The prototype design is made under the geometric constraints imposed by the rectangular NdFeB magnet material, which is available in 20mm x 10mm x 1mm. This geometric constraint becomes the benchmark for selecting the size of the rotor and stator diameters. The single-phase stator winding is installed between 2 slotless and coreless acrylic discs with eight poles. The two acrylic discs used have different diameters, where the first disc with a diameter of 5mm is used as a place to install the windings, and the second disc with a diameter of 1mm is used as a cover. Both are reinforced with several bolts to attach the stator winding firmly. The use of acrylic instead of copper eliminates eddy current losses. In addition, the cost of making stator slots, heat losses, and linear current density can be considered as design inputs.

The analytical procedure for designing a layered rectangular magnet is based on the equivalent approximation of a magnetic circuit to an electric circuit. Fig. 3 shows the equivalent of "electrical circuit" and "magnetic circuit," which is one approach method that can help provide an overview of magnetic phenomena. This circuit diagram shows that "electrical circuit" and "magnetic circuit" are equivalent. Therefore the mathematical relationship of the two circuits is also the same.

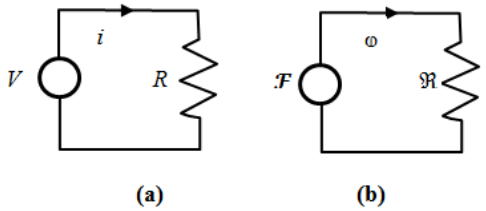

Fig. 3. (a) Electric circuit equivalent and (b) Magnetic circuit analog

Based on Fig. 3, there are some similarities/equivalence parameters between electric circuits and magnetic circuits as given in Table 2.

Table 2. The analogy of quantity of electric circuit and magnetic circuit

Circuit		Units	
Electric	Magnetic	Electric	Magnetic
Voltage *(v)*	Magnetic force *(F=Ni)*	Volt	Amp-turns
Current *(i)*	Magnetic flux (*φ*)	Ampere	Webers, Wb
Resistance *(R)*	Reluctance *(ℜ)*	Ohm	Amp-turns/Wb
Conductivity *(1/ρ)*	Permeability *(μ)*	Mho	Wb/A.t.m
Current density *(J)*	Magnetic flux density *(B)*	A/m^2	Wb/m^2 = teslas T
Electric field *(E)*	Magnetic field intensity *(H)*	Newton/Coulomb (N/C)	Amp-turn/m

Equation (1) is identical to Ohm's Law:

$$I = \frac{V}{R} \quad (15)$$

For a magnetic circuit, the desired effect is flux (φ), while the cause of the magnetic force ($\mathscr{F}$) is the external force (pressure) required to determine the magnetic flux lines in a magnetic material. The resistance to flux determination (φ) is reluctance ($\Re$), the value of the above equation is given by:

$$\varphi = \frac{\mathcal{F}}{\Re} \quad (16)$$

Using Kirchhoff's voltage law "cause" analogy, the equation can be obtained:

$$\sum_0 \mathcal{F} = 0 \quad \text{(Untuk rangkaian listrik)} \tag{17}$$

This equation states that the sum of the algebraic increases and decreases in the magnetic force around a closed loop in a magnetic circuit is zero. The increase in the magnetic force is equal to the amount of decrease in the magnetic force around the closed-loop. This condition is expressed in an equation called Ampere's Circuit Law. If this equation is applied to a magnetic circuit, then the magnetic force is denoted by:

$$\mathcal{F} = N\,I \quad \text{(At)} \tag{18}$$

4. Configuration of the AFPM Generator

Fig. 4 shows a prototype AFPM generator configuration with a simple design consisting of one rotor disk (Fig. 4a) and one stator disk (Fig. 4c) separated by an air gap (δ). The total turbine cost is perhaps the most important criterion for rural electrification applications in developing countries.

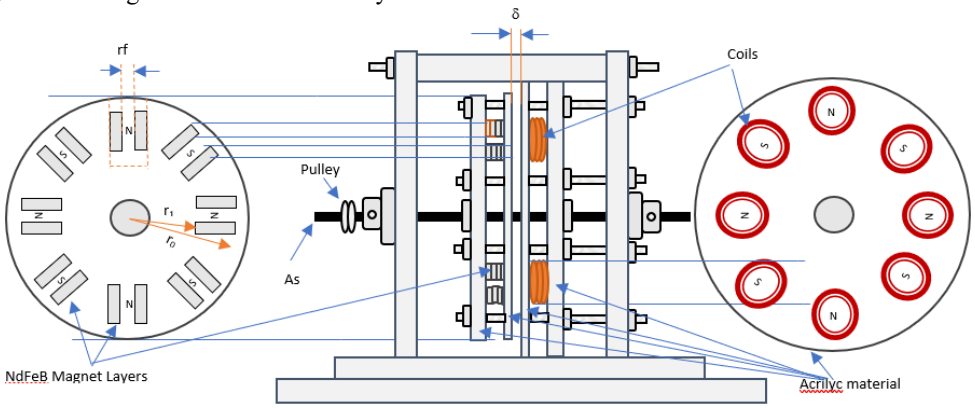

Fig. 4. The AFPM generator prototype: (a) Rotor disc; (b) The proposed AFPM generator; (c) Stator disc

Experimentally, this research aims to optimize the low-cost design of the acrylic stator and rectangular magnet rotor. For consideration, the acrylic material is used to assemble the stator and rotor of the AFPM generator. In addition to eliminating the effects of iron loss, the acrylic material is strong and resistant to heat exposure. As discussed in [33] regarding studies of ironless couplings, acrylic has very small inertia and can be useful in many applications. The material can eliminate the magnetic saturation effect on the yoke iron. Acrylic is a smooth form with a refractive index of 1.49 and is malleable by heat without losing optical clarity. Acrylic is easy to saw, drill, grind, engrave and cut with a sharp carbide tool.

As shown in Fig. 4, both the stator coil positions and the rotor magnets are slotless. They are held together by two acrylic plates that are secured with long bolts. The rotor position, slot or slotless stator, and winding arrangement provide benefits to machine assembly without creating coil slots and rotor magnet slots. In addition, the easy manufacturing process, the simple structure also provides free air to cool the stator windings and rotor magnets. The choice of using rectangular NdFeB magnets arranged in layers is also a low-cost consideration. Fig. 5 shows a rectangular type of magnet with 20 mm x 10 mm x 1 mm as the magnetic field source in the rotor.

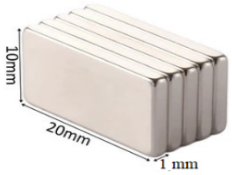

Fig. 5. Rectangular NdFeB magnet

5. Frequency Selection, Number of Poles, Magnetic Type, and Magnetic Flux Measurement

Here, the generator output voltage will be the main concern; the nominal frequency selection will be more relevant considering the total cost of the generator than its operational characteristics. Therefore, the nominal frequency, f_{nom} (frequency at nominal wind speed), determines the number of pole pairs p given by Eq. (1).

$$p = \frac{120 f_{nom}}{N_{nom}} \tag{18}$$

where:

- P = number of poles
- F_{nom} = nominal frequency
- N_{nom} = nominal speed

In the nominal frequency design approach, 50 Hz with a nominal rotation of 750 Rpm, the 8 number of poles is obtained. The permanent magnets used in this design are rectangular NdFeB magnets, the cheapest and available material on the market. In general, wind generator rotor fabrication uses coin magnets, requiring a special installation slot. Rectangular NdFeB magnets are preferred because they are easy to install, appear suitable for this application, and are cheaper than coin magnets.

Even though it has the same volume, the value of rectangular magnetic flux sold in the market is different, so measuring the certainty of the magnetic flux value is to design the stator coil. The use of magnetic teeth on the rotor is carried out in various ways starting from the arrangement of 1 - 4 layers. A Teslameter type WT 110A was used in measuring the average magnetic flux value with 3 repetitions. As seen in Table 3, the measurement results of the overall magnetic flux value for 8 poles are 1.89 T (1 layer), 2.5 T (2 layers), 2.9 T (3 layers), and 3.2 T (4 layers), respectively.

Table 3. Magnetic layer flux measurements

No	1 Layer				2 Layers				3 Layers				4 Layers				Notes
	Measurement to-(mT)				Measurement to-(mT)				Measurement to-(mT)				Measurement to-(mT)				
	1	2	3	$\bar{x}_1$	1	2	3	$\bar{x}_2$	1	2	3	$\bar{x}_3$	1	2	3	$\bar{x}_4$	
1	95	85	90	90	167	176	177	173.3	165	169	171	168.3	191	179	180	183.3	a
	115	115	114	114.7	125	129	126	126.7	159	155	161	158.3	185	187	191	187.7	b
2	120	120	115	118.3	156	156	151	154.3	184	183	184	183.7	190	195	200	195	a
	75	80	80	78.3	122	121	118	120.3	149	147	151	149	198	195	195	196	b
3	165	170	165	166.7	178	178	181	179	213	213	215	214.3	230	230	233	231	a
	145	153	145	147.7	160	162	167	163	195	190	194	193	211	219	220	216.7	b
4	110	110	109	109.7	150	150	154	151.3	193	189	193	191.7	235	241	240	238.7	a
	165	175	165	168.3	178	175	179	177.3	200	200	201	200.3	219	215	215	216.3	b
5	135	133	133	133.7	153	150	153	152	193	187	190	190	209	217	219	215	a
	115	120	115	116.7	154	152	156	154	180	177	180	179	189	189	190	189.3	b
6	110	105	109	108	147	145	148	146.7	175	169	169	171	195	193	195	194.3	a
	110	95	99	98	134	137	142	137.7	184	177	189	183.3	205	199	204	202.7	b
7	110	115	114	113	147	145	151	147.7	165	167	165	165.7	189	184	185	186	a
	115	110	113	112.7	140	140	143	141	173	171	173	172.3	191	185	190	188.7	b
8	110	107	105	107.3	141	141	136	139.3	180	180	179	179.7	193	193	193	193	a
	105	105	104	104.7	130	130	133	131	203	195	203	200.3	203	209	209	207	b
$\sum x_T$			X_1= 1,887				X_2= 2,494				X_3= 2,899				X_4= 3,241		

6. Design of Generator Coils

When the generator rotates, it will cause magnetic flux due to changes in the generator's magnetic field. The maximum magnetic flux or maximum magnetic flux density can be determined by Eq. (7). The basis for designing the stator windings of the AFPM generator is 8 poles, the number of turns per pole is calculated using Eq. (11). By using the maximum flux value of 8 rectangular magnetic poles of 1.89 T, the length of the magnet is 20 mm, and the air gap distance of 1 mm is obtained:

$$B_{max} = 1.89\ x\ \frac{0.02}{0.02+0.01} = 1.8\ T$$

With Eq. (8) and (9), the maximum flux value of the magnetic area in the rotor is obtained:

$$A_m = \frac{3.14\ (0.08^2 - 0.06^2) - 0.035\ (0.08 - 0.06)\ x\ 8}{8}$$

$$= 3.99 \times 10^{-4}\ m^2$$

$$\emptyset_{max} = 3.99\ .\ 10^{-4} \times 1.8 = 7.182 \times 10^{-4}\ \text{weber}$$

$$N = \frac{E}{4{,}44\ x\ f\ x\ K_{w1} x\ \Phi}$$

$$N = \frac{15}{4{,}44\ x\ 50\ x\ 0.8 x\ 7.182\ x\ 10^{-4}} = 117\ turns$$

Based on these results, 117 stator coils were assembled per pole using copper wire with a diameter of 0.3 mm. The characteristics of the generator output voltage are also tested based on variations in the number of stator windings and magnetic layers. In this paper, we have tested the addition of 2 times the initial design with 324 turns. Fig. 6 shows the design of the stator coil mounted on an acrylic material.

7. Disc of the Rotor Magnet

The disc magnet rotor is made of acrylic material with a thickness of 8 mm with a diameter of 20 mm, as shown in Fig. 7. Great attention is paid to the magnetic installation composition different from the existing magnetic rotor models. After selecting the most cost-effective commercial magnets suitable for this application, the magnets are aligned and layered. There are 2 magnets installed parallel with a distance of 3.5 cm on one pole. The experiment is carried out by arranging magnets in layers (parallel) starting from 1 - 4 layers from each 8 poles magnet placement. The goal is to see the effect of the output voltage characteristics of the APFM generator. It can be seen that the use of rectangular magnets is 16 pieces (1 layer), 32 pieces (2 layers), 48 pieces (3 layers), and 56 layers (4 layers), respectively. Keep in mind that once the magnets are attached, the rotor discs will face each other with the stator windings, and in this position, each magnet will be facing a magnet of opposite polarity. The two discs attract each other and thus create the necessary magnetic circuit. Adjustment of the air gap between 1 to 4 mm is also carried out to determine the flux effect's characteristics that interact between the stator and rotor.

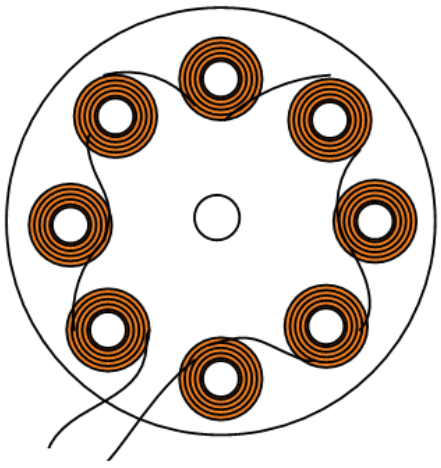

Fig. 6. Stator coils design

8. Experimental results

As mentioned earlier, some of the main problems encountered during the manufacturing and design process are cost, rotor disc material, rotor magnet type. This latter problem has replaced the coin sectoral type magnet with a rectangular magnet that is properly aligned in a single disc rotor magnet. In addition, the placement of the stator coil without a slot

around the acrylic disc. The clear facts show AFPM generator fabrication is easy to manufacture and simple construction. The construction results mentioned above and design problems and their influence on the overall generator performance were tested under laboratory conditions (Fig. 8). The generator is driven by a variable speed DC motor from 100 - 1500 Rpm. Measurement of the output voltage of a no-load APFM generator to determine the voltage characteristics. The 1 - 4 mm air gap variation is regulated and regulates the magnetic flux interaction between the rotor and stator.

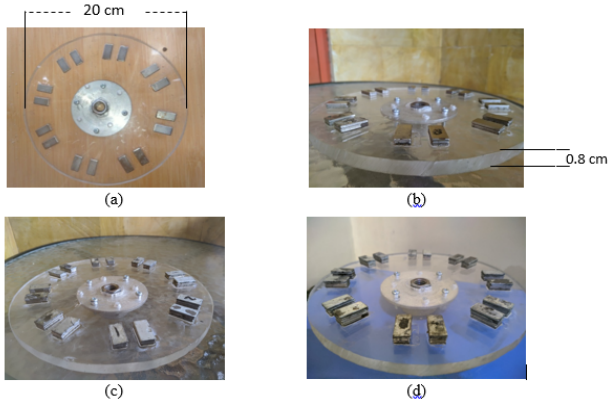

Fig. 7. Rotor design: (a) 1 layer; (b) 2 layers; (c) 3 layers; (d) 4 layers

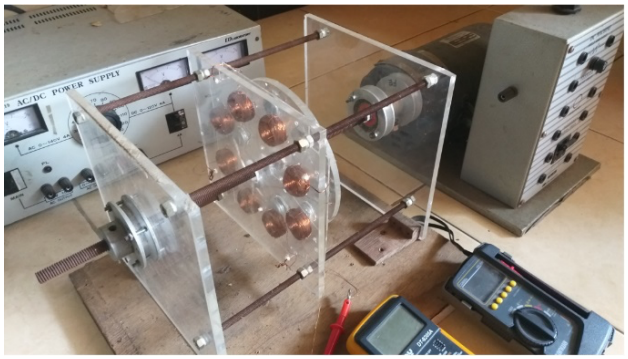

Fig. 8. Prototype machine in the test bench

The no-load generator output voltage (V_o vs. RPM) test results are plotted in the graph, as shown in Fig. 9. By adjusting the rotation from 400 - 1400 Rpm, the maximum output voltage for each magnetic layer variation is 2.68 Volts (1 layer), 3.4 volts. (2 layers), 4.2 Volt (3 layers) and 5.6 Volt (4 layers). An increase in the output voltage is obtained at the change in the number of stator windings by increasing 2 times from 117 turns to 234 turns, as shown in Fig. 10. The result is a voltage of 4.24 Volt (1 layer), 8.4 Volt (2 layers), 11.7 Volt (3) layers) and 13.1 Volt (4 layers).

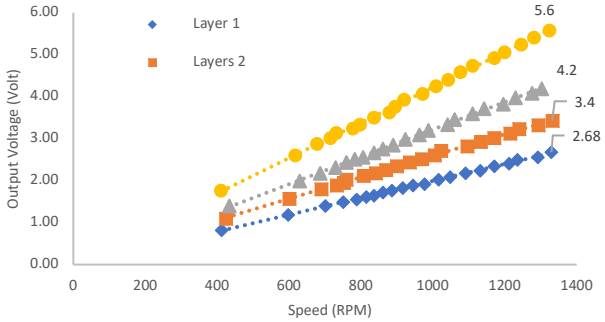

Fig. 9. Output voltage vs speed (117 turns)

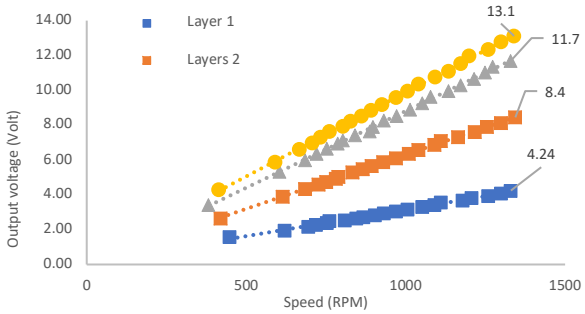

Fig. 10. Output voltage vs speed (234 turns)

This experiment was also carried out to determine the effect of the air gap on the APFM generator output voltage. As already mentioned, the air gap variation is set from 1 - 4 mm, and the resulting graph plot is shown in Fig. 11. It can be seen that the air gap setting affects the output voltage. According to Yao et al. [34], the 1 mm distance between the two magnetic gears is ideal for transferring high torque rotations. The torque will decrease in proportion to the increase in the air gap distance, and when the air gap increases to a certain level, the torque decreases [35].

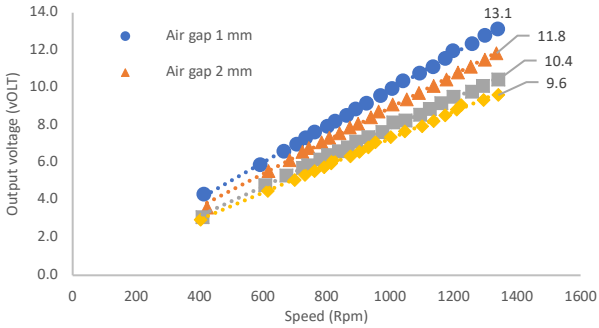

Fig. 11. Effects of air gap on output voltage

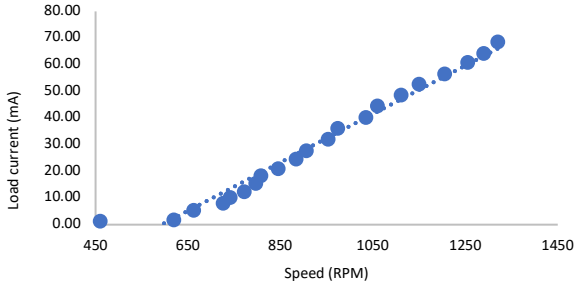

Fig. 12. Load current vs. speed

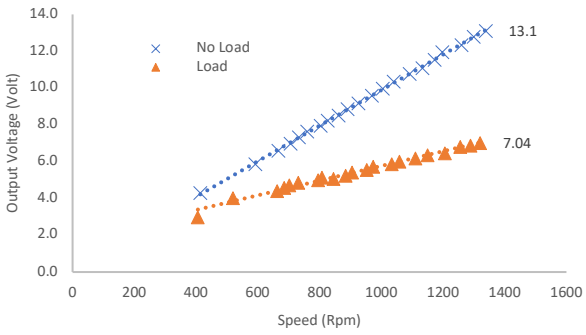

Fig 13. Output voltage (no load vs. load)

The rated load current and the ratio of the no-load and load output voltages according to speed change (RPM) are reported in Fig. 12 and Fig. 13, respectively. Due to the load

applied to the generator, the speed change is proportional to the decrease in the output voltage. Laboratory testing shows the satisfactory thermal operation of the generator while producing nominal power for a long time. Regarding the operation of the generator, it turned out that the EMF voltage was lower than expected. That is due to poor transmission belt systems used, such as slips. As a result, there are heat and friction losses, which cause a decrease in the generator's output power. The generator runs smoothly when measured in open circuit operation without producing sound or acoustic vibrations. The same thing is observed when the generator is connected to a DC lamp load. Some deviations from the theoretical equations describe the diode bridge rectifier's uncontrolled operation and thus some deviations from the measured output voltage. In the unloaded condition, the output voltage is 13.1 volts, and in different conditions, using a diode bridge rectifier has a voltage drop of 7.04 volts.

9. Discussion

AFPM machines have been used for several years in various applications, the most prominent of which are wind generators and electric vehicles. The AFPM generator is particularly suited for such an application since it can be designed with a large pole number and a high torque density. According to [36], in terms of energy yield, reliability, and maintenance, the direct-drive generator system for wind turbines is better than the geared generator system. Direct drive generators operate at low speeds, so a generator with high tangential forces and large air gap diameters is required for sizeable direct-drive wind turbines [37]. These requirements make large direct-drive wind generators heavy and expensive [38, 39]. Therefore, the cost-effectiveness of large direct-drive generators for wind turbines is essential.

This problem was overcome by designing a more straightforward AFPM generator with rectangular magnets and cheaper stator and rotor materials. In this paper, the design of this generator has been made simpler, without an iron core, lighter because it uses acrylic material instead of iron. In addition, experimental tests have been carried out on air gaps 1-4 mm wider as a condition for operating low-speed wind generators. Changes in the wider air gap cause a decrease in the generator output voltage. That requires an optimal air gap setting to obtain the maximum output voltage from the AFPM generator. In contrast, adding the stator winding allows increasing the voltage for more significant output power requirements.

On the other hand, Cavagnino et al. [40] have reported that axial flux engines have higher torque densities than their counterparts based on radial flux. The comparison procedure uses simple thermal considerations for the same overall volume. The actual losses per unit surface wasted, the same air gap, gears, yoke flux density, and rotational speed of the two machine structures, which gave rise to the influence of pole number, were also considered. The advantages of AFPM engine torque density are increasingly visible in designs with many poles.

10. Conclusions

Overview of the design and manufacturing process of the slot-less AFPM generator with carefully arranged rectangular magnets for small-scale wind turbines with direct models. These processes have proven to be easy to implement while enabling the transfer of technology applications in the context of rural electrification. This locally produced small wind turbine features a proven design and robust manufacturing process using acrylic materials in the stator and rotor fabrication. This process can be easily understood with just basic scientific knowledge. They can also be modified by users and the technicians who set them up to meet local needs and use local materials. These facts form the basis for building open-source small wind turbine hardware that can provide electrification to rural communities at lower costs and empower local communities with the technical know-how on creating renewable energy sources. This work can be extended by adjusting the magnet gear using a longer or wider magnet size with a higher flux value to obtain a larger output voltage.

Acknowledgment

The authors would like to acknowledge the Laboratory of Electrical Engineering, University of Nusa Cendana - Kupang, and funds support from the Ministry of Research and Technology funded this research in the Higher Education Excellence Applied Research Grant with contract number 138/UN15.19.1.2/SP2H/LT/2020.

References

1. Parviainen, A., Niemela, M., Pyrhonen, J., and Mantere, L.J. Performance comparison between low-speed axial-flux and radial-flux permanent magnet machines including mechanical constraints. IEEE Int. Electric Machines and Drives Conf., IEMDC (2005).
2. Holmes, A.S., Hong, G., and Pullen, K.R. Axial-flux permanent magnet machines for micro power generation. J. Microelectromech System, 14(1): 54–62 (2005).
3. Chen, Y., Pillay, P., and Khan, A. PM wind generator topologies. IEEE Transactions on Industry Applications, 41: 1619-1626 (2005).
4. Dubois, M.R., Polinder, H., and Ferreira, J.A. Comparison of generator topologies for direct-drive turbines, IEEE Nordic Workshop on Power and Industrial Electronics (2000).
5. Sitapati, K., and Krishman, R. Performance comparisons of radial and axial field, permanent-magnet, brushless machines, IEEE Transactions on Industry Applications, 37: 1219-1226 (2001).
6. Cavagnino, A., Lazzari, M., Profumo, F., and Tenconi, A. A comparison between the axial flux and the radial flux structures for PM synchronous motors. IEEE Transactions on Industry Applications, 1517-1524 (2002).
7. Bumpy, J.R., and Martin, R. Axial-flux permanent-magnet air-cored generator for small scale wind turbines, IEE Proc. Electr. Power Appl., 152(5): 1065-1075 (2005).
8. Muljadi, E., Butterfield, C.P., and Wan, Y.H. Axial flux modular permanent-magnet generator with a toroidal winding for wind turbine applications. IEEE Trans. Ind. Appl., 35(4): 831-836 (1999).
9. Chan, T. F., and Lai, L. L. An axial-flux permanent-magnet synchronous generator for a direct-coupled wind-turbine system. IEEE Trans. Energy Conv., 22(1): 86-94 (2007).
10. Kamper, M. J., Wang, R. J., and Rossouw, F.G. Analysis and performance of axial flux permanent-magnet machine with air-cored non overlapping concentrated stator windings. IEEE Trans. Industry Applications, 44(5): 1495-1504 (2008).

11. Parviainen, A., Pyrhonen, J., and Kontkanen, P. Axial flux permanent magnet generator with concentrated winding for small wind power applications. IEEE International Conference on Electric Machines and Drives. 1187-1191 (2005).
12. Brown, N., Haydock, L., and Bumby, J. R. Foresight vehicle: A toroidal, axial flux generator for hybrid IC engine/battery electric vehicle applications. Proc. SAE Conf. paper 2002-01-089.
13. Spooner, E., and Chalmers, B. J. (1992). TORUS, A slotless, toroidal-stator permanent magnet generator. IEE Proc. Electr. Power Appl. 497–506 (2002).
14. Huang, S., Aydin, M., and Lipo, T. A. TORUS concept machines: pre-prototyping design assessment for two major topologies. IEEE Industry Applications Conf., 3(30): 1619–125 (2001).
15. Spooner, E., and Chalmers, B. J. TORUS, A toroidal-stator, iron poles rotor permanent magnet machine for small scale power generation. International Conf. on Electrical Machines.1053-1058 (1990).
16. Dostal, Z., Lipo, T. A., and Chalmers, B. J. Influence of current waveshape on motoring performance of the slotless permanent magnet machine TORUS, International Conf. on Electrical Machines and Drives. 376-380 (1993).
17. Chalmers, B. J., Green, A. M., Reece, A. B. J., and Al-Badi, A. H. Modeling and simulation of the TORUS generator. IEE Proceedings on Electric Power Applications, 144(6): 446-452 (1997).
18. Wu, W., Spooner, E., and Chalmers, B. J. Design of slotless TORUS generators with reduced voltage regulation. Proc. IEEE, Electric Power Application, 142(5): 337-343 (1995).
19. Boccaletti, C., Elia, S., and Nisticò, E. Deterministic and stochastic optimisation algorithms in conventional design of axial flux PM machines, Int. Symposium on Power Electronics, Electrical Drives, Automation and Motion, Speedam. 111-115 (2006).
20. Aydin, M., Huang, S., and Lipo, T. A. Optimum design and 3D finite element analysis of non-slotted and slotted internal rotor type axial flux PM disc machines. IEEE PES Summer Meeting, Vancouver, CA (2001).
21. Huang, S., Aydin, M., and Lipo, T. A. Performance assessment of axial flux permanent magnet motors for low noise applications, Final Project Report to Naval Surface Warfare Center, University of Wisconsin-Madison (2000).
22. Huang, S., Aydin, M., and Lipo, T. A. Low noise and smooth torque permanent magnet propulsion motors: Comparison of non-slotted and slotted radial and axial flux topologies. IEEE Int. Aegean Electrical Machine and Power Electronic Conf., Kusadasi-Turkey. 1-8 (2001).
23. Huang, S., Aydin, M., and Lipo, T. A. Torque quality assessment and sizing optimization for surface mounted PM machines. IEEE Industry Applications Society Annual Meeting, Chicago. 1603-1610 (2001).
24. Hill-Cottingham, R. J., Coles, P. C., Eastham, J. F., Profumo, F., Tenconi, A., and Gianolio, G. Multi-disc axial flux stratospheric aircraft propeller drive. IEEE Industry Applications Society Annual Meeting (2001).
25. Piggott. H. A wind turbine recipe book-The axial flux windmill plans (2009).
26. Bumby J. R., Stanard, N., Dominy, J., and McLeod, N. A permanent magnet generator for small scale wind and water turbines. In Proc. of the 2008 International Conference on Electrical Machines; paper 733; p.1 (2008).
27. Mishnaevsky L., Freere, P., Sinha, R., Acharya, P., Shrestha, R., and Manandhar, P. Small wind turbines with timber blades for developing countries: Materials choice, development, installation and experiences, Renewable Energy (2011).
28. Latoufis, K. C., Messinis, G. M., Kotsampopoulos, P. C., and Hatziargyriou, N. D. Axial flux permanent magnet generator design for low-cost manufacturing of small wind turbines. Wind Engineering, 36(4) (2012).
29. Wu, Y.C., and Wang, C.W. Transmitted torque analysis of a magnetic gear mechanism with rectangular magnets. Applied Mathematics & Information Sciences. 1059-1065 (2015).
30. Wu, Y. C., Tseng, W. T., and Chen, Y. C. Torque ripple suppression in an external-meshed magnetic gear train. Advances in Mechanical Engineering (2013).
31. Syam, S., Soeparman S., Widhiyanuriyawan, D., Wahyudi. Comparison of axial magnetic gears based on magnetic composition topology differences. Energies, 11(153): 1-15 (2018).
32. Syam, S., Kurniati, S., Ramang, R. Design and characteristics of axial magnetic gear using rectangular magnet. Journal Europeen des Systemes Automatises, 53(2): 167-175 (2020).
33. Charpentier, J., and Lemarquand, G. Calculation of ironless permanent magnet couplings using semi numerical magnetic pole theory method. Int. J. Comput. Math. Electr. Electron. Eng. 72–89 (2001).
34. Yao, Y. D., Chiou, G. J., Huang, D. R., and Wang, S. J. Theoretical computations for the torque of magnetic coupling. IEEE Trans. on Magnetics, 31(3) (1995).
35. Huang, J., Wanga, D., and Zhangb, D. The torque characteristic analysis and simulation on electromagnetic gears. Energy Procedia. 1274 – 1280 (2012).
36. Li H, and Chen Z. Design Optimization and Site Matching of Direct-Drive Permanent Magnet Wind Power Generator Systems. Renewable Energy, 34(4): 1175-1184 (2009).
37. Chan T.F., and Lai L. L. An axial-flux permanent-magnet synchronous generator for a direct-coupled wind-turbine system. IEEE Trans. Energy Conversion. 22(1): 86-94 (2007).
38. Curiac P., and Do-Hyun K. Preliminary evaluation of a megawatt-class low-speed axial flux PMSM with self-magnetization function of the armature coils. IEEE Trans. Energy Conversion, 22(3): 621-628 (2007).
39. Polinder H., van-der-Pijl F. F. A., de-Vilder G. J., Tavner P. J. Comparison of direct-drive and geared generator concepts for wind turbines. IEEE Trans. Energy Conversion. 21(3): 725-733 (2006).
40. Cavagnino A., Lazzari M., Profumo F., Tenconi A. A comparison between the axial flux and the radial flux structures for pm synchronous motors. IEEE Trans. Ind. Appl., 38(6): 1517-1524 (2002).